


Limit analysis of masonry structures with free discontinuities

A. Fortunato · F. Fabbrocino · M. Angelillo · F. Fraternali 

Received: 6 September 2016 / Accepted: 17 March 2017
© Springer Science+Business Media Dordrecht 2017

Abstract We formulate a novel procedure for the limit analysis of two-dimensional masonry structures subject to arbitrary loading conditions. The proposed approach works in the framework of free discontinuity methods, on examining collapse mechanisms that exhibit free crack opening discontinuities. The load bearing capacity and the collapse mechanism of the structure are obtained through a fully variational approach, by minimizing a kinetic functional that admits the collapse crack pattern as a variable. Numerical examples illustrate the practical application of the proposed procedure to the limit analysis of a variety of masonry walls and arches subject to foundation settlements, vertical and horizontal forces.

Keywords Masonry structures · Load bearing capacity · Limit analysis · Kinematic collapse multiplier · Free discontinuities

A. Fortunato · M. Angelillo · F. Fraternali (✉)
Department of Civil Engineering, University of Salerno,
Via Giovanni Paolo II, 132, 84084 Fisciano, SA, Italy
e-mail: a.fortunato@unisa.it

M. Angelillo
e-mail: m.angelillo@unisa.it

F. Fraternali
e-mail: f.fraternali@unisa.it

F. Fabbrocino
Department of Engineering, Pegaso University, Piazza
Trieste e Trento, 48, 80132 Naples, Italy
e-mail: francesco.fabbrocino@unipegaso.it

1 Introduction

A simplified constitutive model of masonry is the so-called *Normal Rigid No-Tension* (NRNT), which is well suited for structures where the effects of bending and shear stresses on the collapse mechanisms are negligible [1–9]. More sophisticated constitutive relations for such a material have been proposed in the literature, with the aim of capturing the actual inhomogeneous nature of masonry, and complex behaviors frequently observed under experimental tests, such as softening-type response, time-dependent phenomena, friction, linear and nonlinear homogenization (refer, e.g., to [10–14] and references therein). As observed in the introductory article of the recent book [9], the real geometry and the material properties of most masonry buildings are not known in detail, so that the definition of even the most primitive engineering parameters, such as strength and stiffness, might be difficult and affected by high randomness and uncertainty. One of the most basic constitutive assumption that can be made for masonry, in view of the small and often erratic value of the tensile strength, is that the material can carry only compressive stresses (No-Tension/NT model). Since the pioneering work of Heyman [1] it is generally recognized that such an assumption leads to a powerful and meaningful interpretation of the fracture patterns exhibited by a wide class of real masonry structures.

Several authors of the Italian school of structural mechanics have studied and enriched the NT model over the years, through a variety of mathematical, numerical and experimental approaches (see, e.g., Refs. [3–9]). By way of examples and through mathematical arguments, it has been shown that the study of the ultimate load-carrying capacity of masonry structures can be conducted within the framework of the limit analysis of solid bodies, by estimating lower (safe theorem) and upper (kinematic theorem) bounds of the collapse load, in presence of suitable admissible stress and strain fields (cf. [15, 16]). The use of singular stress and strain fields within the static and kinematic theorems of the limit analysis of masonry structures is diffusely reviewed in [17, 18]. Typically, the above discontinuities are ‘a-priori’ introduced along pre-defined patterns, which usually coincide with the edges of suitable finite element discretizations of the body to be analyzed.

The present work generalizes such an approach, by dealing with a free-discontinuity formulation of the kinematic theorem of limit analysis of masonry structures in two-dimensions. We examine collapse mechanisms that exhibit singular strain fields representing concentrated fractures, on extending a previous free-discontinuity model of the elastic problem of masonry structures [19] based on the variational formulation of Griffith-type fracture in brittle solids [20]. It is worth noting that free discontinuities approaches to plasticity and rigid-block problems of limit analysis have been proposed in Refs. [21–23] over recent years. The free-discontinuity model presented in this work approaches the functional of the kinematically admissible collapse multiplier of a masonry body by taking the crack pattern as a variable of the problem. On minimizing such a functional over a discrete set of collapse mechanisms with crack-opening displacements, and employing a numerical model with movable interfaces separating rigid elements, we seek for a local minimum point of the above functional. As a result we predict both the collapse load and the collapse mechanism of the body through a fully variational approach, which does not require the pre-definition of the crack pattern. The practical implementation of the proposed approach is illustrated through a collection of numerical examples dealing with masonry structures subject to both vertical and horizontal forces.

2 The boundary value problem for rigid no-tension materials

2.1 Constitutive restrictions and equilibrium problem

We consider a body $\Omega \in \mathbb{R}^n$ (here $n = 2$), loaded by the given tractions \underline{s} on the part $\partial\Omega_N$ of the boundary, and subject to given displacements \underline{u} on the complementary, constrained part of the boundary $\partial\Omega_D$, is in equilibrium under the action of such given surface displacements and tractions, besides body loads \mathbf{b} and distortions \underline{E} [the set of data being denoted: $(\underline{u}, \underline{E}; \underline{s}, \mathbf{b})$], and undergoes small displacements \mathbf{u} and strains $\mathbf{E}(\mathbf{u})$.¹

The body Ω is composed of a Rigid No-Tension (RNT) material, that is the stress \mathbf{T} is negative semidefinite

$$\mathbf{T} \in \text{Sym}^-, \tag{1}$$

the effective strain $\mathbf{E}^* = \mathbf{E}(\mathbf{u}) - \underline{E}$ is positive semidefinite

$$\mathbf{E}^* \in \text{Sym}^+, \tag{2}$$

and the stress \mathbf{T} does no work for the corresponding effective strain \mathbf{E}^*

$$\mathbf{T} \cdot \mathbf{E}^* = 0. \tag{3}$$

2.2 Admissible fields

For RNT materials is natural to define the sets of statically admissible stress fields \mathcal{H} and kinematically admissible displacement fields \mathcal{K} , as follows

$$\mathcal{H} = \{ \mathbf{T} \in \mathcal{S}(\Omega) \text{ s.t. } \text{div}\mathbf{T} + \mathbf{b} = \mathbf{0}, \mathbf{T}\mathbf{n} = \underline{s} \text{ on } \partial\Omega_N, \mathbf{T} \in \text{Sym}^- \}, \tag{4}$$

$$\mathcal{K} = \{ \mathbf{u} \in \mathcal{T}(\Omega) \text{ s.t. } \mathbf{u} = \underline{u} \text{ on } \partial\Omega_D, (\mathbf{E}(\mathbf{u}) - \underline{E}) \in \text{Sym}^+ \}, \tag{5}$$

where a convenient choice for the function spaces $\mathcal{S}(\Omega)$ and $\mathcal{T}(\Omega)$ is

¹ When eigenstrains are considered, under the small strain assumption, the total strain $\mathbf{E}(\mathbf{u})$ is decomposed additively as follows: $\mathbf{E}(\mathbf{u}) = \mathbf{E}^* + \underline{E}$, \mathbf{E}^* being the *effective* strain of the material.

$$\begin{aligned} \mathcal{S}(\Omega) &= SMF(\Omega), \\ \mathcal{T}(\Omega) &= \{\mathbf{u}, \text{s.t. } \text{grad } \mathbf{u} \in SMF^*(\Omega)\}, \end{aligned} \tag{6}$$

$SMF(\Omega)$ being the set of special measures (that is measures with null Cantor part) whose jump set is finite, in the sense that the support of their singular part consists of a finite number of regular $(n - 1)$ d arcs. With $SMF^*(\Omega)$ we denote the subset of $SMF(\Omega)$ for which the support of the singular part is restricted to a finite number of $(n - 1)$ d segments.

3 Compatibility conditions

3.1 Compatibility and incompatibility of loads and distortions

The data of a general BVP for a RNT body can be split into two parts

$$\begin{aligned} \ell &\leftrightarrow (\underline{\mathbf{s}}, \mathbf{b}) \approx \text{loads}, \\ \ell^* &\leftrightarrow (\underline{\mathbf{u}}, \underline{\mathbf{E}}) \approx \text{distortions}. \end{aligned} \tag{7}$$

The *equilibrium problem* and the *kinematical problem* for RNT materials, namely the search of admissible stress or displacement fields for given data, are essentially independent, in the sense that they are uncoupled but for condition (3).

It has to be pointed out that, for RNT bodies, there are non-trivial compatibility conditions, both on the loads and on the distortions; that is the existence of statically admissible stress fields for given loads, and the existence of kinematically admissible displacement fields for given distortions, is submitted to special conditions on the data (for a thorough study of compatibility conditions on the loads see [7]).

The definition of compatible loads and distortions is rather straightforward:

$$\begin{aligned} \{\ell \text{ is compatible}\} &\Leftrightarrow \{\mathcal{H} \neq \emptyset\}, \\ \{\ell^* \text{ is compatible}\} &\Leftrightarrow \{\mathcal{K} \neq \emptyset\}. \end{aligned} \tag{8}$$

Therefore the more direct way to prove compatibility, both for loads and distortions, is to construct a s.a. stress field or a k.a. displacement field, as done in the previous examples.

To prove the existence of a solution to the BVP for a No-Tension body, the compatibility of ℓ and ℓ^* is necessary but not sufficient, since the further condition

$$\mathbf{T} \cdot \mathbf{E}^*(\mathbf{u}) = 0, \tag{9}$$

must be satisfied (this is the material restriction (3)). Then one can say that a possible solution to the BVP is given, if there exist a s.a. stress field and a k.a. displacement field, which are reconcilable in the sense of condition (3).

The way to verify the incompatibility of the data is less straightforward.

$$\{\ell \text{ incompatible}\} \Leftarrow \{\exists \mathbf{u}^0 \in \mathcal{H}^0 \text{ s.t. } \langle \ell, \mathbf{u}^0 \rangle > 0\}, \tag{10}$$

$$\{\ell^* \text{ incompatible}\} \Leftarrow \{\exists \mathbf{T}^0 \in \mathcal{H}^0 \text{ s.t. } \langle \ell^*, \mathbf{T}^0 \rangle > 0\}, \tag{11}$$

where \mathcal{H}^0 and \mathcal{K}^0 are the same as defined in (4) and (5) but with set of data $(\underline{\mathbf{u}}, \underline{\mathbf{E}}; \underline{\mathbf{s}}, \mathbf{b}) = (\mathbf{0}, \mathbf{0}; \mathbf{0}, \mathbf{0})$, and $\langle \ell, \mathbf{u}^0 \rangle, \langle \ell^*, \mathbf{T}^0 \rangle$ represent the work of the loads and distortions for $\mathbf{u}^0, \mathbf{T}^0$, respectively.

4 Limit analysis

We concentrate on necessary or sufficient conditions for the compatibility of a given set of loads $(\underline{\mathbf{s}}, \mathbf{b})$, restricting to the case of zero kinematical data $(\underline{\mathbf{u}}, \underline{\mathbf{E}})$.

4.1 Theorems of limit analysis

Strictly admissible stress fields and load classification

On denoting $\langle \ell, \mathbf{u} \rangle$ the work of the load $\ell = (\underline{\mathbf{s}}, \mathbf{b})$ for the displacement \mathbf{u} , the load can be classified as follows:

$$(\ell \text{ is a collapse load}) \Leftrightarrow (\exists \mathbf{u}^* \in \mathcal{H} \text{ s.t. } \langle \ell, \mathbf{u}^* \rangle > 0) \tag{12}$$

$$\begin{aligned} (\ell \text{ is a limit load}) &\Leftrightarrow (\langle \ell, \mathbf{u} \rangle \leq 0, \forall \mathbf{u} \in \mathcal{H} \text{ and } \exists \mathbf{u}^* \\ &\in \mathcal{H} - \mathcal{H}^{00} \text{ s.t. } \langle \ell, \mathbf{u}^* \rangle = 0) \end{aligned} \tag{13}$$

$$(\ell \text{ is a safe load}) \Leftrightarrow (\langle \ell, \mathbf{u} \rangle < 0, \forall \mathbf{u} \in \mathcal{H}) \tag{14}$$

where \mathcal{H}^{00} and \mathcal{K}^{00} are the sets \mathcal{H}^0 and \mathcal{K}^0 corresponding to null stress and strain fields, depending on the geometry of the boundary, of the loads and of the constraints. A stress field $\mathbf{T} \in \mathcal{H}$ such that $\text{tr}\mathbf{T} < 0$ and $\text{def}\mathbf{T} > 0, \forall \mathbf{x} \in \Omega$, is said to be *strictly admissible*.

Notice that, if \mathbf{T} is strictly admissible, then at each point of Ω (that is the open set $\dot{\Omega}$ to which the fixed part of the boundary $\partial\Omega_D$ is added) it results: $\sigma_1 < 0, \sigma_2 < 0, \sigma_1, \sigma_2$ being the eigenvalues of \mathbf{T} at the point \mathbf{x} .

Kinematic Theorem If ℓ is a collapse load (in the sense of item (1) above) then \mathcal{H} is void.

Static Theorem If a strictly admissible stress field \mathbf{T} exists, then the load ℓ is safe (in the sense of item (3) above).

Limit Theorem If \mathcal{H} is not void and there exists $\mathbf{u}^* \in \mathcal{H} - \mathcal{H}^{00}$ such that $\langle \ell, \mathbf{u}^* \rangle = 0$, then the load ℓ is limit (in the sense of item (2) above).

For the proof of these theorems we refer to the paper [15]. The reader must be warned that the proofs given by Del Piero refer to a similar function space for the displacement but to a different functional setting for the stress (namely $L^2(\Omega)$). In the present paper we assume that these theorem are still valid in the present larger setting for the stress.

4.2 Formalization of the kinematical problem

We focus on the formalization of the kinematical problem under the effect of kinematical data (such as settlements and distortions). By restricting to displacement fields characterized by strain fields that are, purely, line Dirac deltas with support on a finite number of segments, the body Ω can be divided into a finite number, say n , of domains Ω_i (forming a partition of Ω) each exhibiting a rigid body motion. Under the assumption of small strains, for each element Ω_i , such rigid body motion, that is the displacement \mathbf{u}^i of any point of Ω_i , can be described in terms of three displacement parameters u^i, v^i, ϕ^i , as follows

$$u_1^i(x_1, x_2) = u^i - \phi^i x_2, \quad u_2^i(x_1, x_2) = v^i + \phi^i x_1. \tag{15}$$

Under these restrictive assumptions the generalized displacement of the structure, denoted $\hat{\mathbf{u}}$ is a vector of $3n$ components, namely the three displacement parameters per each element Ω_i :

$$\hat{\mathbf{u}} = \{u^1, v^1, \phi^1, \dots, u^i, v^i, \phi^i, \dots, u^n, v^n, \phi^n\}. \tag{16}$$

5 A free-discontinuity approach to kinematic collapse analysis

The present study is concerned with masonry structures composed of rigid no-tension material, that is a continuum for which the stress and strain are restricted by the assumptions (1), (2), (3). In Fig. 1 the main idea is depicted for a simple plane wall with regular openings: thick solid lines represent the boundary; thin solid lines represent fixed interfaces; grey lines represent moving interfaces. We formulate a *free-discontinuity approach* to the kinematic collapse analysis of a masonry body by letting the separation interfaces be free to move within the reference configuration, through suitable, *configurational* movements of their end nodes (Fig. 1).

The unilateral constraint considered along the interfaces, incorporates the no-penetration condition. The normality condition (2), (3) (that is the non-sliding assumption along the interface) is enforced by the bilateral pendulum (see Fig. 1b). The kinematical and statical problems for such a structure are coupled, in the sense that, given the assumption of zero dissipation on any interface (Assumption (3)), the work of the reactions for the displacements both at the internal and at the boundary interfaces must be zero. In

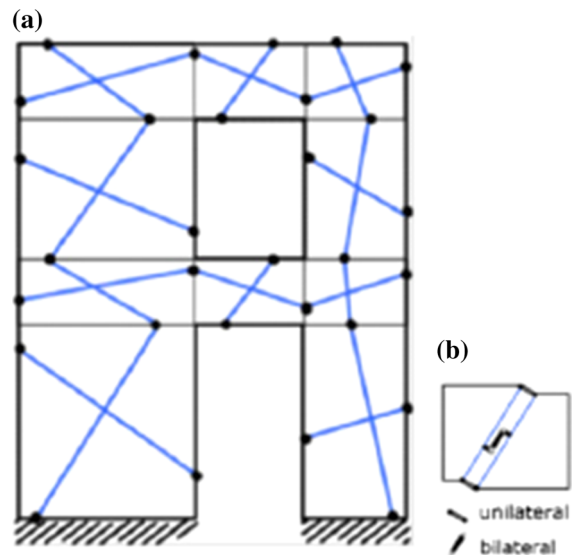


Fig. 1 The rigid-block masonry model with fixed and floating interface

general there will be infinite elements $\hat{u} \in \mathcal{K}$ and infinite elements $\hat{R} \in \mathcal{H}$, and the no-work assumption gives a criterion to select (may be not uniquely), among them, a couple (\hat{u}^0, \hat{R}^0) , that is called: solution of the kinematical and statical problem. (Notice that, restricting to a finite number of rigid blocks, having fixed or moving interfaces, the sets \mathcal{H} and \mathcal{K} become finite dimensional). There is a way to select variationally such a couple. The idea is to introduce the potential energy of the structure, that is minus the potential energy of the loads, i.e. the scalar product of the loads and couples applied at the centroids of the pieces, collected in a generalized force vector \hat{f} , for the generalized displacement \hat{u} collecting the parameters of translation and rotation of each piece of S). We call the potential energy $E(\hat{u})$, and minimize $E(\hat{u})$ over the set \mathcal{K} . We write

$$E(\hat{u}) = -\langle \hat{f}, \hat{u} \rangle, \tag{17}$$

as a linear function of the generalized displacement u of the structure, and set

$$E(\hat{u}^0) = \min_{\hat{u} \in \mathcal{K}} E(\hat{u}). \tag{18}$$

This is a linearly constrained minimization problem for a linear function if the interfaces are not moving, that is the pieces are fixed. In such a simplified case the problem can be solved by using Linear programming (e.g., the simplex method). If both the load data and the distortion data are fixed, the minimum criterion selects, among all the kinematically admissible displacements \hat{u} the displacement \hat{u}^0 that is more convenient on an energetically ground. If the load is assigned with a load parameter λ (say: the vertical component of the load is fixed and the horizontal component is gradually increased with λ), at each stage of the loading program (that is at any given value of λ) the minimal displacement can be calculated through the minimum condition. The limit value λ^0 of the load parameter is obtained when a mechanism (that is an indefinite increase of the displacement) for which the loads perform zero work is detected. Our free-discontinuity approach allows the separation discontinuities to move within the reference configuration of the body, on employing the two-stage minimization algorithm that is illustrated in Sects. 6.2 and 6.3.

6 Numerical results

6.1 A case study with fixed discontinuities

As a first case study, we analyze the case study depicted in Fig. 2, which is concerned with the façade wall of a XVII century building from the archive of the Italian National Fire Corps, section of Bergamo (courtesy of Prof. Paolo Faccio, IUAV Venezia), exhibiting a widespread crack pattern due to a differential settlement of the foundation. We model the portion of the wall interested by the foundation settlement as a set S of $n = 7368$ triangular rigid blocks connected by unilateral and bilateral constraints (Fig. 3). The profile of the applied settlements is given in Fig. 3a on adopting a magnification factor equal to 4. An arbitrary generalized displacement of the wall is given by

$$\hat{u} = \{u(1), v(1), \phi(1), \dots, u(n), v(n), \phi(n)\}. \tag{19}$$

with the displacement parameters being referred to the centroid of the mesh elements. The corresponding generalized dual force is as follows

$$\hat{F} = \{H(1), V(1), M(1), \dots, H(n), V(n), M(n)\}. \tag{20}$$

Assuming pure dead loads due to the self-weight of the wall, we have: $H(i) = 0, V(i) = P(i), M(i) = 0$, for any $i = 1, 2, \dots, n$, where $P(i)$ is the self-weight of the panel i . The bilateral and unilateral constraints depicted in Fig. 1b are considered to be active on all the mesh interfaces, which leads us to the following system of equality and inequality constraints:

$$\Gamma' \hat{u} = 0, \quad \Gamma'' \hat{u} \leq \delta, \tag{21}$$

δ being the vector of the applied settlements. The set of kinematically admissible generalized displacement is given by

$$\mathcal{K} = \{\hat{u} : \Gamma' \hat{u} = 0, \Gamma'' \hat{u} \leq \delta\}, \tag{22}$$

and the crack pattern \hat{u}^0 is numerically obtained by minimizing the objective function

$$E(\hat{u}) = -\hat{F} \cdot \hat{u} \tag{23}$$

over \mathcal{K} . The result provided in Fig. 3b shows an overall good matching between our prediction of the crack pattern of the wall, and the real pattern

Fig. 2 The façade of a XVII century building exhibiting a manifest crack pattern due to a foundation settlement (courtesy of Prof. Paolo Faccio, IUAV Venezia)



illustrated in Fig. 2. Due to the large number of unknowns and constraints, an interior point algorithm was employed to minimize the objective function (23).

6.2 Collapse mechanism with free-discontinuities of a barrel vault subject to seismic loading

A second example deals with the collapse analysis of the monumental barrel vault structure shown in Fig. 4a. The loading condition is represented by the self-weight p of the structure (masonry unit weight equal to 17 KN/m^3), and horizontal forces λp (static seismic loading, cf. Fig. 4a). We estimate the collapse multiplier of the horizontal forces by analyzing a 1.0 m long slice of the structure, and discretizing such a region through the r-adaptive mesh shown in Fig. 4b. Such a mesh is obtained by nesting a discontinuous mesh (dashed red edges) into a continuous mesh (solid black edges). The nodes of the discontinuous mesh are allowed to move along the edges of the fixed mesh, giving rise to an adaptive discontinuous triangulation [20]. We obtain a free-discontinuity estimate of the collapse multiplier λ_c through a two-level minimization procedure. Let ξ_i the scalar variable ranging in the interval $(-1, 1)$ that defines the position of the generic movable node of the discontinuous mesh. We set $\xi_i = \pm 1$ when such a node is ‘collapsed’ at the nodes of the continuous edge along which it is constrained to move. Let ξ denote the vector collecting the ξ_i variables of all the movable nodes. For a given vector ξ collecting the

position variables of all the movable nodes ξ_i , we minimize the following functional

$$E(\hat{u}, \xi) = -\hat{f} \cdot \hat{u} \tag{24}$$

over the set \mathcal{K} of all the admissible generalized displacements \hat{u} that are allowed to exhibit separation discontinuities along the edges of the discontinuous mesh. Here, \hat{f} defines the generalized force vector collecting both vertical forces (self-weight), and horizontal forces proportional to the load multiplier λ (Fig. 4a). The above minimization is performed through a standard linear programming algorithm, and returns a load multiplier that we interpret as the ‘fitness’ function λ^0 of the given ξ . Next, we minimize $\lambda^0(\xi)$ under the bound constraints $-1 < \xi_i < 1$, via the evolutionary algorithm illustrated in [24], on obtaining a ‘free-discontinuity’ collapse multiplier λ_c . Figure 4c shows the collapse mechanism obtained for the present example through the adaptive discontinuous mesh in Fig. 4b ($\lambda_c = 0.1053$). It is worth noting that such a mechanism features four opening hinges (cracks) in the masonry, one of which is located in a buttress and the other three over the vault.

6.3 Collapse mechanism with free-discontinuities of a masonry wall with openings subject to seismic loading

Our final example is concerned with a three-story wall with openings under the action of fixed vertical loads,

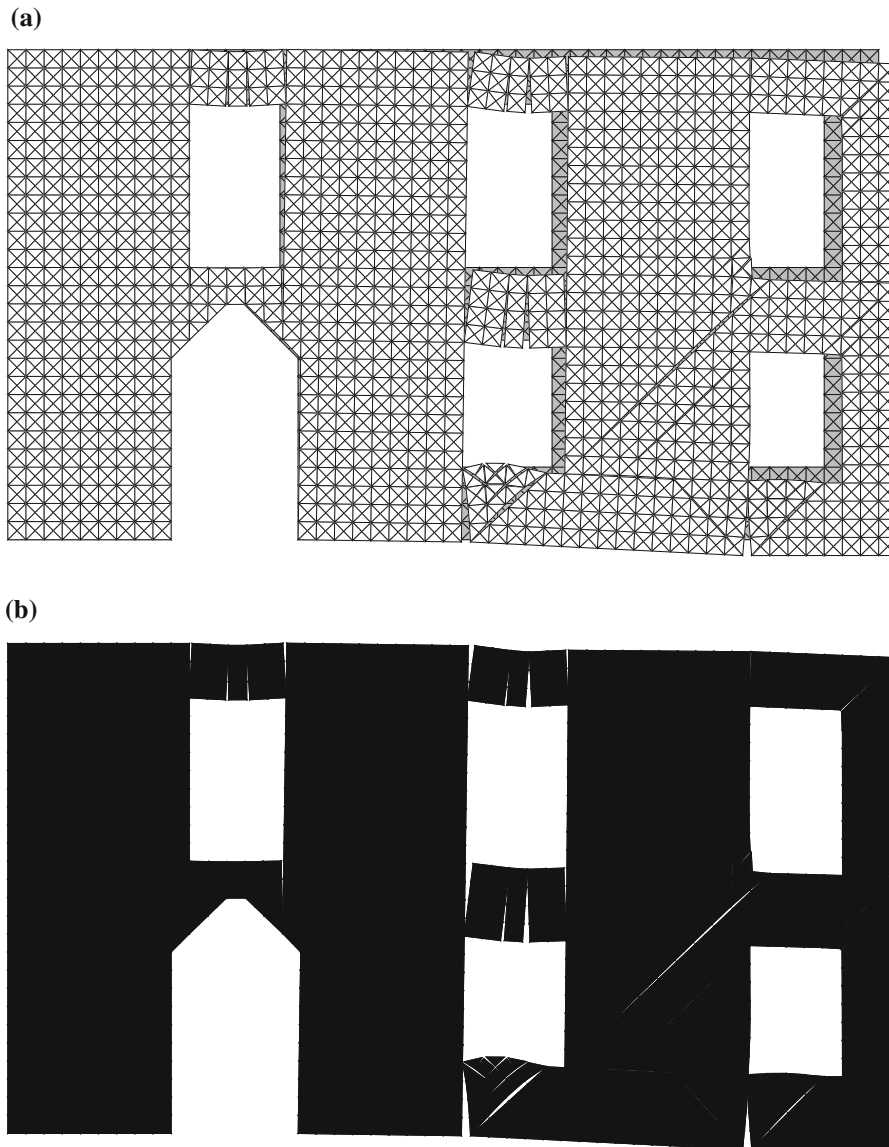


Fig. 3 Crack pattern of façade wall with openings due to a given ground settlement: **a** superimposed original and deformed configurations; **b** silhouette of the deformed configuration highlighting the crack pattern

and horizontal forces that grow from base values $F_1 = 33.82$ kN; $F_2 = 45.58$ kN; $F_3 = 70.31$ kN proportionally to a load multiplier λ (Fig. 5a). The masonry is made of 1.0 m thick tufo bricks featuring 18 kN/m³ self-weight. Distributed vertical loads with magnitude 7.5 kN/m are applied at each story level. We solve such an example through the procedure described in the previous section, on employing the mesh shown in Fig. 5b. Such a mesh shows r-adaptive nodes in correspondence with the diagonals crossing

the masonry blocks (potential crack-opening discontinuities), which are allowed to move along one of the competent diagonals. We solve the current example through the two-level minimization procedure described in the previous section, by governing the movement of the adaptive nodes through a configurational variables $-1 < \zeta_i < 1$. Figure 5b shows the final collapse mechanism predicted obtained for the structure under examination, which corresponds to $\lambda_c = 3.9827$.

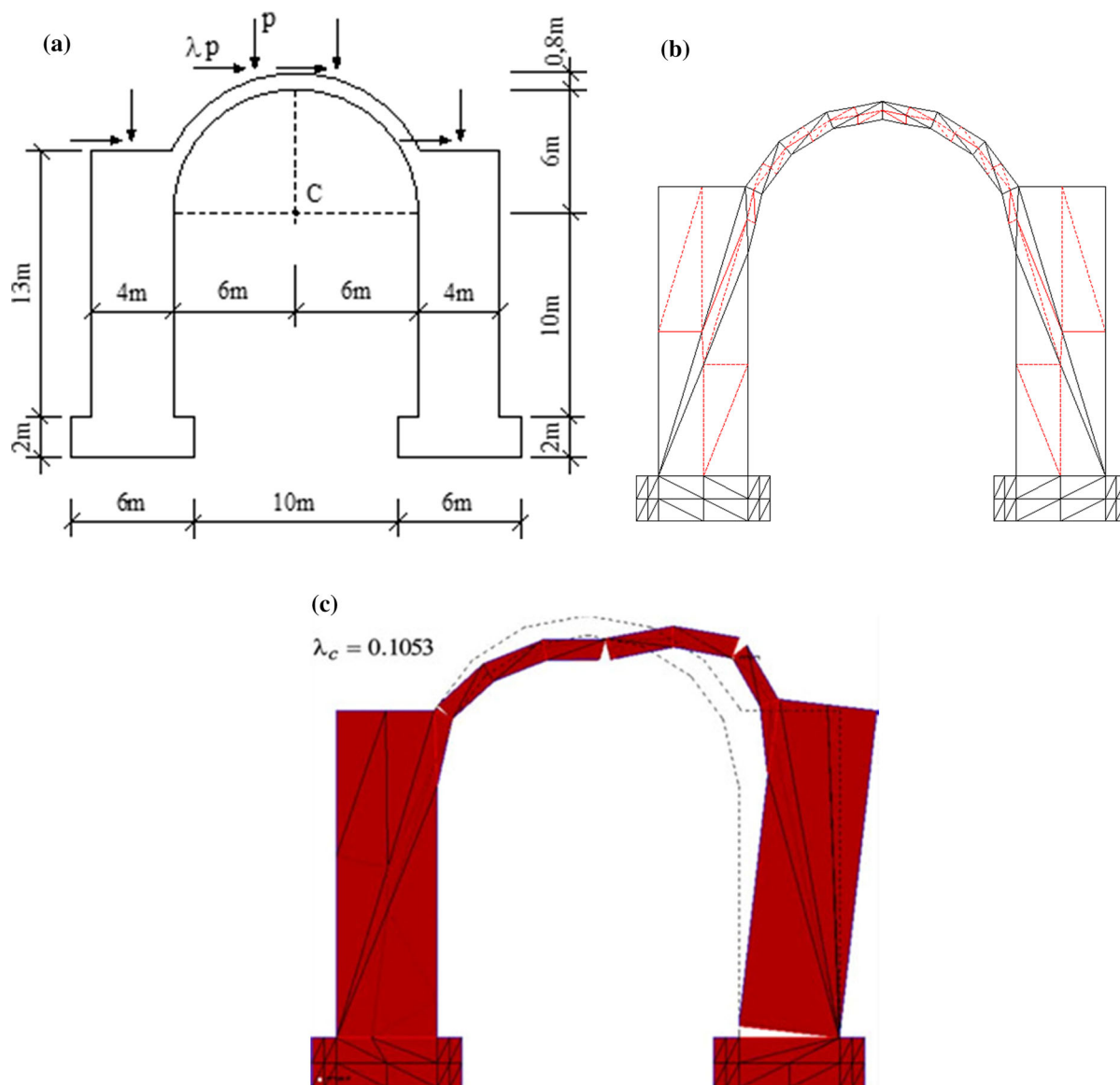


Fig. 4 Masonry structure covered with a barrel vault (a), adopted mesh featuring r-adaptive separation surfaces (*dashed red lines*) (b), and predicted collapse mechanism (c)

7 Concluding remarks

The free-discontinuity model presented in this work can be used to predict the ultimate load carrying capacity of arbitrary 2D masonry structures under vertical and horizontal loads, with the latter describing seismic excitations within a conventional static approach [25]. It returns the collapse multiplier and the collapse mechanism of the structure under investigation through a fully variational procedure, which

does not require any a-priori assumption on the crack pattern exhibited by the structure at collapse. A two-level minimization procedure has been adopted to search for the collapse multiplier of discontinuous finite element models that are equipped with rigid blocks and r-adaptive separation interfaces. It is worth remarking that the given procedure can be easily extended to 3D structures with no conceptual difficulties, but just a greater computational burden. It provides an accurate tool for predicting the actual

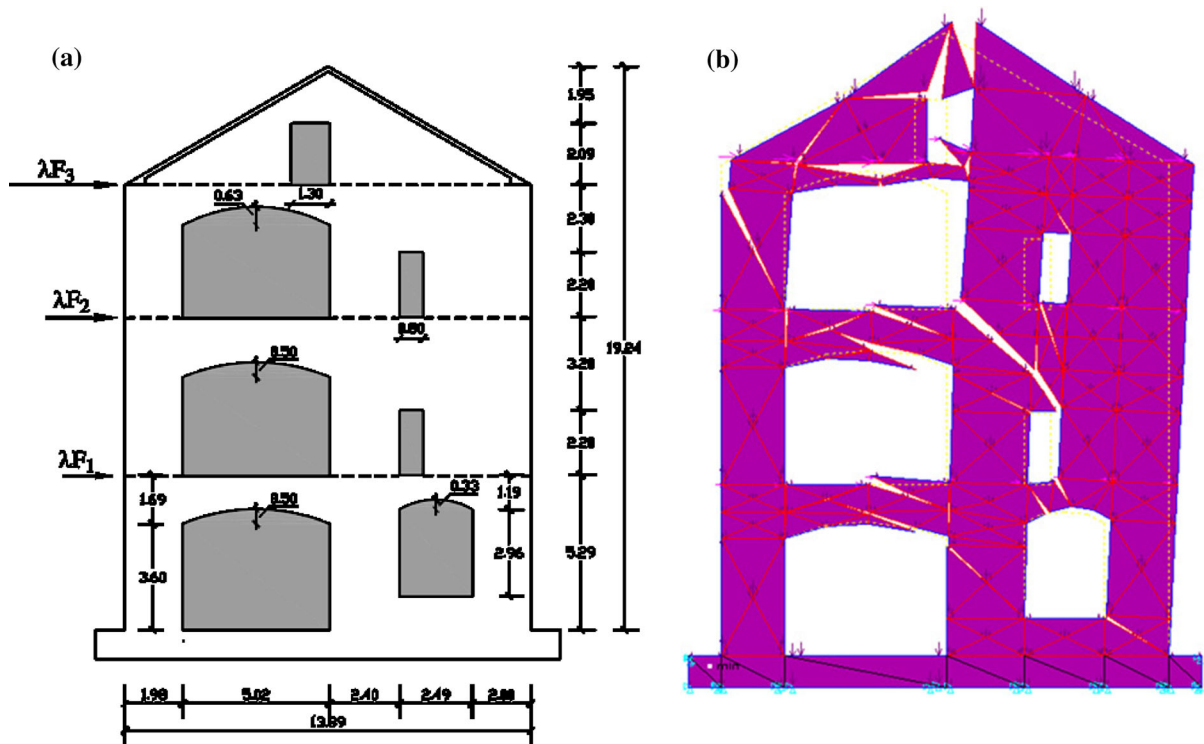


Fig. 5 Masonry wall with openings subjected to fixed vertical loads and variable horizontal forces: **a** geometry and loading scheme; **b** predicted collapse mechanism

collapse mechanism of real masonry structures under seismic actions, which represents a major problem in all the countries (like, e.g. Italy) that are interested by severe earthquakes and exhibit rich and precious historical heritage constructions.

It is worth noting that the numerical procedure for the limit analysis of masonry structures here proposed is based on a recursive *linear programming* technique, whose computational efficiency relies on the agility of the employed linear minimization procedure. For large-scale problems (more than 1 K variables) the basic *simplex method* (exponential running time) should be replaced by more efficient tools, such as, e.g., the interior point method, which runs in polynomial time. On observing, for the sake of example, that the number of bricks in a traditional masonry building of four storeys and planar dimensions of about 20 m × 20 m is roughly 10⁶, we can expect this numerical limit being barely an issue with running time of few minutes for a model equipped with appropriate macro rigid elements [22, 23].

Future extensions of the present study will focus on the limit behavior of masonry walls, vaults, and 3D structural complexes featuring arbitrarily complex

shapes [26]. Additional future research lines might regard the generalization of the current free-discontinuity approach to masonry structures reinforced through traditional and/or composite materials, on accounting for interface debonding and ripping at the interfaces between masonry and reinforcements [27, 28].

Acknowledgements The authors wish to thank Antonino Iannuzzo from the Department of Structures for Engineering and Architecture of the University of Naples ‘Federico II’ for his helpful assistance with the numerical results presented in Sect. 6.1.

Compliance with ethical standards

Conflict of interest The authors declare that they have no conflict of interest to report.

References

1. Heyman J (1966) The stone skeleton. *Int J Solids Struct* 2:249–279
2. Como M, Grimaldi A (1985) A unilateral model for the limit analysis of masonry walls. In: Del Piero G, Maceri F (eds) *Unilateral problems in structural analysis*. CISM courses and lectures. Springer, Berlin, pp 25–45

3. Di Pasquale S (1984) *Statica dei solidi murari*. Atti Dipartimento Costruzioni. University of Firenze, Florence, Italy
4. Romano G, Romano M (1979) Sulla soluzione di problemi strutturali in presenza di legami costitutivi unilaterali. *Rendiconti Accademia Nazionale dei Lincei* 67:104–113
5. Baratta A, Toscano R (1982) Stati tensionali in pannelli di materiale non resistente a trazione. In: *Proceedings VI AIMETA Congress*, Genova
6. Giaquinta M, Giusti E (1985) Researches on the equilibrium of masonry structures. *Arch Ration Mech Anal* 88:359–392
7. Del Piero G (1989) Constitutive equation and compatibility of the external loads for linear elastic masonry-like materials. *Meccanica* 24:150–162
8. Como M (1992) Equilibrium and collapse of masonry bodies. *Meccanica* 27(3):185–194
9. Angelillo M (ed) (2014) *Mechanics of masonry structures*. Series: CISM International Centre for Mechanical Sciences, vol 551. Springer-verlag, Wien
10. Milani G (2012) New trends in the numerical analysis of masonry structures. *Open Civ Eng J* 6:119–120
11. Tralli A, Alessandri C, Milani G (2014) Computational methods for masonry vaults: a review of recent results. *Open Civ Eng J* 8:272–287
12. Gesualdo A, Monaco M (2015) Constitutive behaviour of quasi-brittle materials with anisotropic friction. *Lat Am J Solids Struct* 12(4):695–710
13. Addessi D, Sacco E (2016) Enriched plane state formulation for nonlinear homogenization of in-plane masonry wall. *Meccanica* 51(11):2891–2907
14. Addessi D, Sacco E (2014) A kinematic enriched plane state formulation for the analysis of masonry panels. *Eur J Mech A Solids* 44:188–200
15. Del Piero G (1998) Limit analysis and no-tension materials. *Int J Plast* 14:259–271
16. Fraldi M, Nunziante L, Gesualdo A, Guarracino F (2010) On the bounding of multipliers for combined loading. *Proc R Soc A Math Phys Eng Sci* 466(2114):493–514
17. Block P, Ochsendorf J (2007) Thrust network analysis: a new methodology for three-dimensional equilibrium. *J Int Assoc Shell Spat Struct* 48(3):167–173
18. Fraternali F (2010) A thrust network approach to the equilibrium problem of unreinforced masonry vaults via polyhedral stress functions. *Mech Res Commun* 37:198–204
19. Angelillo M, Fortunato A, Lippiello M, Montanino A (2014) Singular stress fields for masonry walls: Derand was right. *Meccanica* 49(5):1243–1262
20. Fraternali F (2007) Free discontinuity finite element models in two-dimensions for in-plane crack problems. *Theor Appl Fract Mech* 47:274–282
21. Hawksbee S, Smith C, Gilbert M (2013) Application of discontinuity layout optimization to three-dimensional plasticity problems. *Proc R Soc A Math Phys Eng Sci* 469:20130009
22. Chiozzi A, Milani G, Tralli A (2016) Fast kinematic limit analysis of FRP reinforced masonry vaults through a new genetic algorithm Nurbs-based approach. In: *Proceedings of the ECCOMAS congress 2016, Crete, Greece, 05–10 June*
23. Chiozzi A, Milani G, Grillanda N, Tralli A (2016) An adaptive procedure for the limit analysis of FRP reinforced masonry vaults and applications. *Am J Eng Appl Sci* 9(3):735–745
24. Ascione L, Feo L, Fraternali F, Fraternali F, Marini A, El Sayed T, Della Cioppa A (2011) On the structural shape optimization via variational methods and evolutionary algorithms. *Mech Adv Mater Struct* 18:225–243
25. European Committee for Standardization (2014) *Eurocode 8: design of structures for earthquake resistance. Part 1: general rules, seismic actions and rules for buildings*. EN 1998-1:2004, Brussels, Belgium
26. Angelillo M (2015) Static analysis of a Guastavino helical stair as a layered masonry shell. *Compos Struct* 119:298–304
27. Lang AF, Benzoni G (2014) Modeling of nonlinear behavior of confined masonry using discrete elements. In: *NCEE 2014—10th U.S. national conference on earthquake engineering: frontiers of earthquake engineering*
28. Carpentieri G, Modano M, Fabbrocino F, Feo L, Fraternali F (2017) On a tensegrity approach to the minimal mass reinforcement of masonry structures with arbitrary shape. *Meccanica* 52(7):1561–1576